ELECTRON STORAGE RING AS A SINGLE SHOT LINAC BEAM MONITOR*

Y. Shoji#, K. Takeda, University of Hyogo, Ako 678-1205, Japan
Y. Minagawa, Y. Takemura, S. Suzuki, T. Asaka, JASRI, Sayo 679-5198, Japan

Abstract

The SPring-8 linac has been used as an injector to the electron storage ring, NewSUBARU. There exists a shot-to-shot fluctuation in the injection efficiency during top-up operation. In order to understand the source of the fluctuation, we have developed single shot diagnostics of the injected beam using the visible light beam line of the ring. The techniques utilized the phase rotation of betatron or synchrotron oscillation in the ring. The time-resolving visible light monitor in the ring, a streak camera or ICCD gated camera, records the profiles of the injected linac beam over multiple revolutions. The time profile recorded at the point of injection reveals the bunch structure in the 1 ns macro pulse, which contains three linac bunches. The time profile at after 1/4 of the synchrotron oscillation period gives the energy profile of a pulse. The bunch-by-bunch spatial profiles over consecutive several revolutions after the injection can be used to reconstruct the transverse emittance of each bunch.

INTRODUCTION

The electron storage ring NewSUBARU [1] has used the SPring-8 linac [2] as an injector for top-up operation since 1998. However, fine parameter tuning is required for stable injection because of the small ring acceptance. For that process, single shot linac beam monitors were necessary to measure beam parameters with the injection efficiency. Although the feedback control of steering magnets using BPMs along the transport line [3] improved the stability, the injection efficiency still fluctuates due to the injected linac beam. We have developed single shot diagnostics utilizing the phase rotation in the ring, providing an opportunity to understand fluctuations in the injection efficiency.

We used the time resolving visible light profile monitors of the electron storage ring. The time profile at the instance of the injection, recorded by a streak camera, gives the bunch structure in a pulse. The time profile after 1/4 of the synchrotron oscillation period gives the energy profile. The dual sweep streak camera can also be used to record the spatial profile of several turns. The fast sweep separated linac bunches in a macro pulse and the slow sweep separated profiles from different turn numbers. The betatron oscillation in the ring produced a phase rotation allowing the reconstruction of the beam emittance. Here the beam emittance means not only the area but the ellipse in the transverse phase space.

The stability of the linac beam was evaluated from the shot-to-shot variation. We could also see differences of beam parameters in the bunches of the same macro pulse.

The measurements detailed here required dedicated time at the facility because the stored beam should not exist in the ring. This meant that storage of the injected beam was not necessary. The ring parameters, such as the beta functions, betatron tunes, etc. could be fully optimized for the measurement. This also means that a booster synchrotron of any facility can be used as a monitor if it has a light extraction port.

In addition to the two aforementioned monitors, we will discuss the possibility of using an ICCD gated camera, capable of recording several spatial profiles, allowing analysis of the H/V coupling of the injected beam.

PARAMETERS OF DAILY OPERATION

Averaged Beam Parameters

Figure 1 shows the layout of the SPring-8 linac, the booster synchrotron, and NewSUBARU storage ring. Table 1 shows the main parameters for the linac.

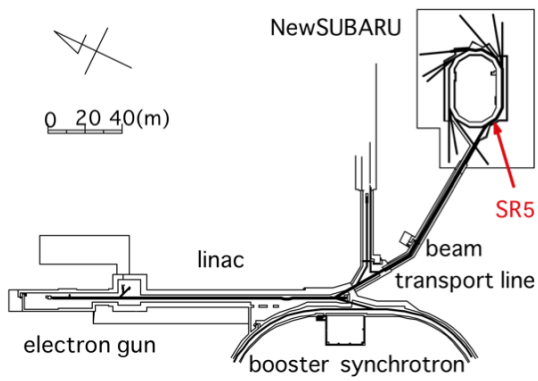

Figure 1: Layout of the 1 GeV SPring-8 linac, the booster synchrotron, and the NewSUBARU storage ring.

Table 1: Main Parameters of the Linac

Electron energy	1 GeV
Rf frequency	2856 MHz
Common pulse rate	1 Hz
Common pulse width	1 ns
FWHM Bunch length; front/middle	10 ps / 14ps
Full energy spread; front / middle	0.4% / 0.6%
Transverse emittance (FWHM^2)	100 π nmrad.

*Work supported by "comprehensive support program for the promotion of accelerator science and technology" by KEK.
shoji@lasti.u-hyogo.ac.jp

ISBN 978-3-95450-119-9

The macro pulse width of the linac beam is normally 1 ns, which enables a single rf bucket injection of the ring, covering three rf buckets of the linac [4]. The 1 ns beam is obtained by applying 200V rectangular pulse to the grid of the thermionic electron gun.

The listed transverse emittance in Table 1 was calculated from the average over many shots, measured by Q-scanning at the beam transport line. The longitudinal parameters were obtained from the measurements of the synchrotron oscillation in the ring just after the injection [5]. The listed bunch length and the energy spread were obtained from the average of 10 shots.

Setup of the Visible Light Beam Line

Figure 2 shows the schematic layout near the injection point and the monitor line, named SR5. The dove prism on the line switches transverse measurement axis for the streak camera, in this case we selected the vertical with 90 degrees rotation.

The Twiss parameters at the light source point are β_x = 0.7 m, β_y = 17 m and the dispersion function is η = 0.052 m. The longitudinal and transverse radiation damping time are 12 ms and 22 ms, respectively.

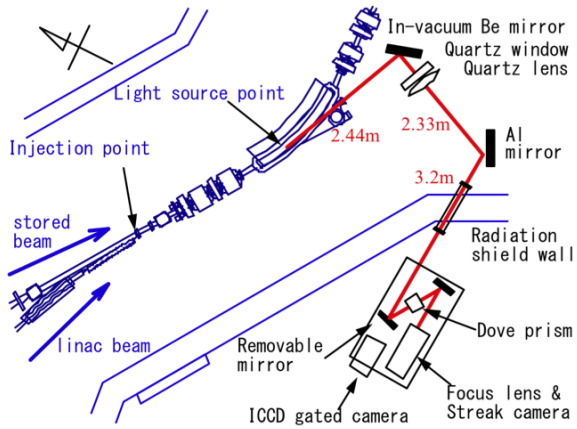

Figure 2: Layout of the visible light monitor line SR5.

CORRELATION OF INJECTION EFFICIENCY WITH BUNCH STRUCTURE

Bunch Structure and Injection Efficiency

The bunch structure was fluctuated by a jittering of the gate pulse timing of the electron gun. Figure 3 shows six typical dual sweep images of the streak camera with six typical bunch structures. They are grouped and named A-F for convenience. The vertical axis in the images is the ring rf phase and the horizontal axis shows the progressively increasing number of revolutions. The time structure at the injection imprints a bunch structure in a pulse. The time profile at 1/4 of the synchrotron oscillation period (41 μs) gives the energy profile.

Figure 4 shows the bunch structure of each group and the corresponding energy profile of the middle bunch. The energy profile had two peaks, separated by 0.3-0.4%. These two peaks were intentionally produced at the bunching process using two bunchers [6].

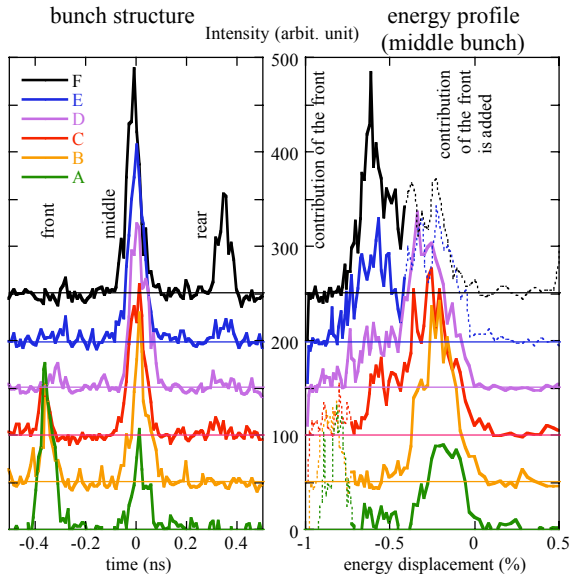

Figure 4: Bunch structure of three bunches and the corresponding energy profile of the middle bunch. The part of the energy profile, that contains a contribution from another bunch was plotted with a dotted line. The labels A-F corresponds to the images of Figure 3.

The injection phase of a bunch was stable with a small jittering of the synchronization system between the 2856 MHz linac rf and the 500 MHz ring rf [7]. On the other hand the timing jitter of the gate pulse was roughly 0.3 ns, much larger than the expected (30 ps FWHM [8]). The actual gate pulse length was thought to be 0.7 ns or less.

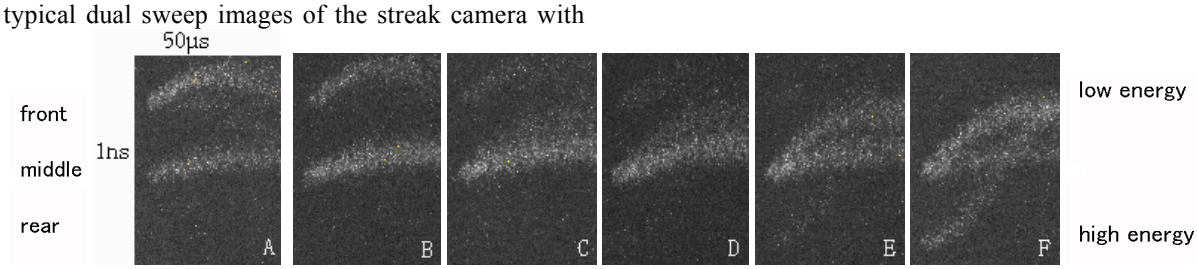

Figure 3: Typical dual sweep images. Because of the non-linear momentum compaction factor, the movement of the front bunch is slower at the initial 50 μs.

ISBN 978-3-95450-119-9

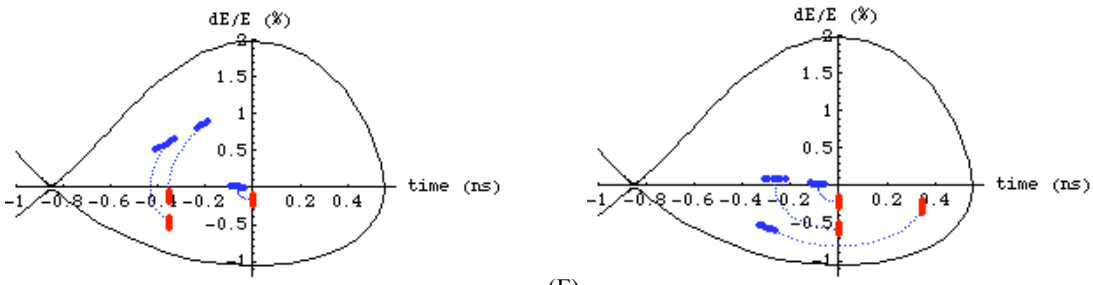

(A) (F)

Figure 5: Calculated movement of bunches in the ring rf bucket for the images A and F of Figure 3. The black solid line is the separatrix. The red spots show the bunches at the injection and the blue spots at after 41 μs. The origin of the time axis is the synchronous phase

Figure 5 shows the movement through 1/4 of the synchrotron oscillation period for images A and F. It explains the non-linear movement in Figure 3. The rf bucket model was based on the measurement of non-linear chromaticity of synchrotron tune [9]. This showed that the acceptance of the rf bucket was large enough for the linac beam. Another experimental survey about the longitudinal ring acceptance was consistent with the model.

Figure 6 shows the injection efficiency of 35 shots with the ring parameters characteristic of daily operation. Shots shown in images A and B had a comparatively worse injection efficiency. These two results suggested that a dependence of transverse parameters caused fluctuations in the injection efficiency.

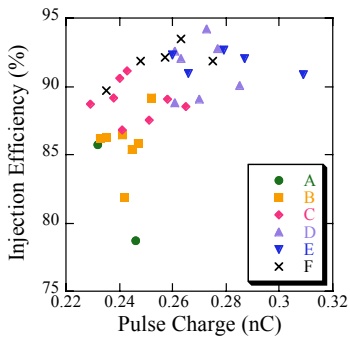

Figure 6: Injection efficiency for different bunch structure labeled A-F in Figure 3.

Here, we will mention that we could have blocked the light from the other bunches at after 41 μs, if we needed accurate energy profile. Setting an appropriate mask at a point of the light source image could have blocked them using a displacement by 0.5% energy difference, although sacrificing the time profile at the injection timing.

BUNCH-BY-BUNCH EMITTAMNCE MEASUREMENT

Setup of the Ring

We wanted a bunch-by-bunch transverse parameter measurement. As the first step, we measured vertical parameters because it was easier than that to measure horizontal parameters.

The linear ring lattice was the same as those of daily operation because the vertical beta function was large at the light source point. Some other parameters were different from those of daily operation during the measurement. The injection pulse bump was optimized so that the injected beam had a small dipole oscillation and maintained almost 100% injection efficiency. The vertical chromaticity was reduced to 0 in order to eliminate the chromatic betatron phase spread over multiple revolutions. The linear H/V coupling was reduced to less than 1%. The very small beam size of the stored beam was used to calibrate the vertical spatial resolution. It was 0.3 mm FWHM at the light source point with $\beta_y = 17$ m.

Data Analysis of a Typical Shot

Here we demonstrate our method of analysis using a representative shot (#12, image B) as an example. Its total charge, measured by fast CT on the beam transport line, was 0.23 nC.

Figure 7 shows the dual sweep image of the streak camera frame and the projection to the fast sweep axis. The vertical axis is the horizontal position in space and the ring rf phase in time. The upper part of the figure corresponds to the head of the linac pulse with the tail in the lower part of the figure. The horizontal axis is the vertical position in space and the ring revolutions in time. The six spots correspnd to profiles from the 4th through 9th turns after the injection. Profiles at the initial 3 turns were out of the camera slit because of a large horizontal displacement. The horizontal profile of each spot in the image corresponds to the vertical spatial profile in the ring.

Figure 8 shows the profiles of the 6 turns of the two respective bunches. They were fitted with Gaussian functions. We derived the peak position y and a divergence σ^2 as a function of the revolution number N.

ISBN 978-3-95450-119-9

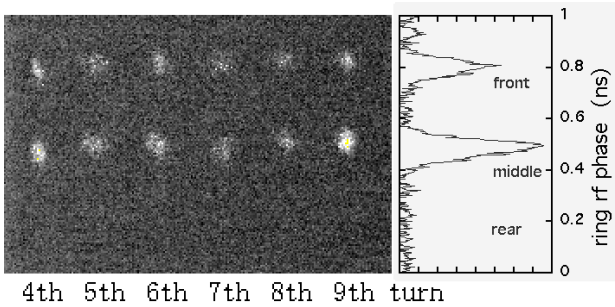

Figure 7: Dual Sweep image of the injected beam of the shot #12.

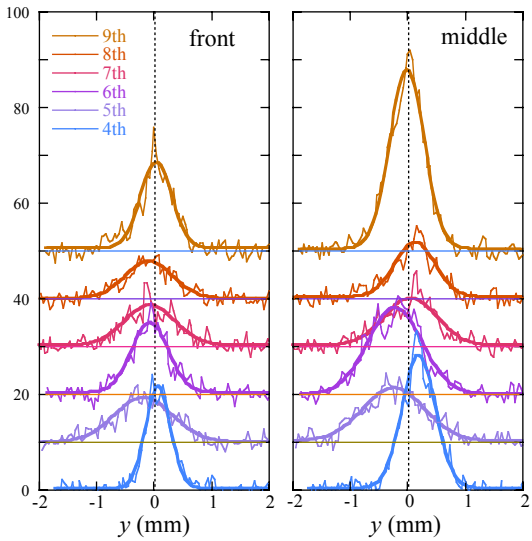

Figure 8: Vertical beam profiles from turns 4 through 9 of the front bunch and the middle bunch.

As shown in Figure 9, the data were fitted with the following sinusoidal functions

$$y = A_0 + A_S \sin(2\pi\Delta\nu_y N) + A_C \cos(2\pi\Delta\nu_y N) \quad (1)$$

$$\sigma^2 = B_0 + B_S \sin(4\pi\Delta\nu_y N) + B_C \cos(4\pi\Delta\nu_y N) \quad (2)$$

Here $\Delta\nu_y$ =0.224 is the sub-integer part of the vertical betatron tune. The dipole oscillations of two bunches were obviously different. The oscillations of the widths were almost the same except for one data point, the 6th turn of the middle bunch.

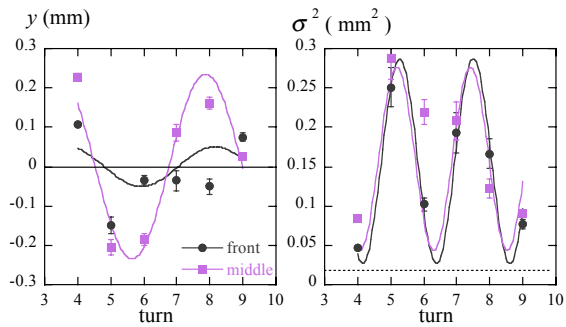

Figure 9: The dipole oscillation of the peak position (left) and the quadrupole oscillation of the divergence (right). The dotted line on the right indicates the spatial resolution.

The beam ellipse at the injection point was calculated using the phase advance to the light source point, 0.15 rad. Figure 10 shows the calculated beam ellipses at the injection point.

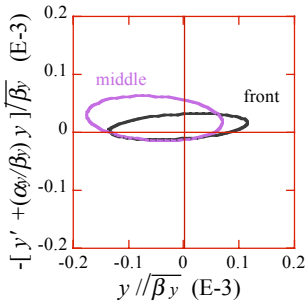

Figure 10: The calculated beam ellipses in the normalized phase space at the injection point.

Shot-to-Shot Fluctuation

We recorded the profiles of 20 shots in order to see the shot-to-shot fluctuation. Figure 11 shows the bunch charge for the 20 shots. They are grouped A-E, according to the charge of the front bunch.

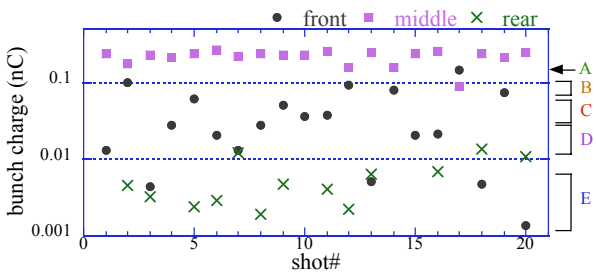

Figure 11: Bunch charge for the highlighted 20 shots.

The parameters quantifying the dipole oscillation, A_C and A_S, of the middle bunch are plotted in Figure 12. The fluctuation was correlated with the group and took place at the phase $\Delta A_S/\Delta A_C$ = 1.3. We added data points of the front bunch of groups A–C to the plot. The differences in the same pulse were roughly of the order of the fluctuation in phase.

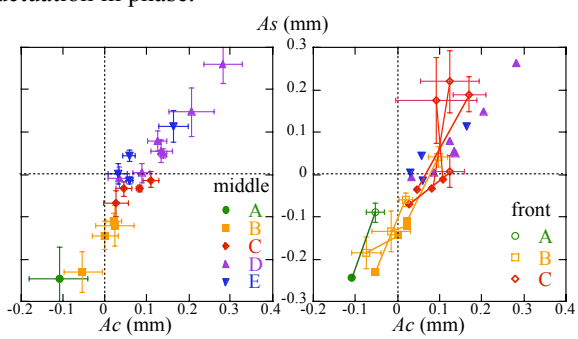

Figure 12: Shot-to-shot fluctuation of the dipole oscillation of the middle bunch (left) and those of the front bunch (right). The oscillations of different bunches in the same shot are connected with lines.

ISBN 978-3-95450-119-9

The parameters for the quadrupole oscillation, B_C and B_S, of the middle bunch are plotted in Figure 13. No clear dependence on the group was observed. However, it seems to be no accident that the difference of two bunches satisfied $2\Delta B_S - \Delta B_C > 0$ for all 8 shots.

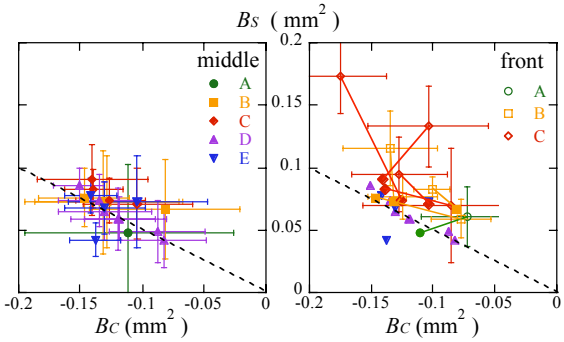

Figure 13: Shot-to-shot fluctuation of the quadrupole oscillation parameters of the middle bunch (left) and those of the front bunch (right).

TRANSVERSE EMITTANCE

At the present, the ICCD gated camera is used to monitor the small transverse oscillation and confirm the identification of the number of revolutions. However it has a potential to reconstruct a transverse four-dimensional profile and identify the H/V coupling of the linac beam. Figure 14 shows an example of single shot profiles from turns two through six in the frame of the ICCD gated camera.

In this case the dipole oscillation was adjusted to a small amplitude. However, an intentional dipole oscillation, both in horizontal and vertical directions, would separate profiles at defferent turns. Too small horizontal beta function at the light source point is the other setting parameters, which should be changed to improve the accuracy of horizontal beam parameters.

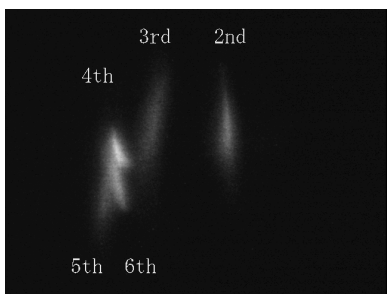

Figure 14: Injected beam profiles from turns two through six taken from the ICCD gated camera.

SUMMARY AND DISCUSSION

We have presented some single shot data from the SPring-8 linac obtained at NewSUBARU. The shot-to-shot fluctuation in the injection efficiency was related to the bunch structure, originating from the time jittering of the gate pulse. The energy profile and the vertical orbit also depended on the bunch structure. The bunch-by-bunch emittance measurement showed a difference in beam parameters for different bunches.

Our measurement showed that the energy stabilization using ECS [8], which certificate the energy stability of 0.02%, is not enough. The improvement of the timing jitter of the grid pulser was another important factor of the beam energy. We are considering to add re-trigger using the master clock for the improvement.

In order to have much injection tolerance, the linac beam energy was raised by 0.4% after the measurements. We are preparing system for the independent tuning of the beam energies, that for the booster and that for NewSUBARU.

The data at our disposal from the new diagnostics provide an opportunity to address and solve problems in a systematic way. However, there still exists scope for improvement. Our research is still underway for more improvement based on better understanding of the injection process.

ACKNOWLEDGMENT

We thank members of the SPring-8 linac group for many suggestions on the measurements and discussions on our results.

The visible light beam line SR5 was constructed under the supervision of Prof. Mitsuhashi of KEK. He aided with the basic design of the beryllium mirror, the measurement of its deformation by synchrotron radiation heat using a Hartmann mask, as well as the elimination of monitor halo from edge scattering.

REFERENCES

[1] A. Ando, *et al.*, *Jour. Synchro. Rad.* **5** (1998) 342.
[2] S. Suzuki, *et al.*, "Recent Improvements in SPring-8 Linac for Early Recovery from Beam Interruption", *LINAC'12*.
[3] K. Yanagida, *et al.*, "Bean Instrumentation Using BPM System of the SPring-8 Linac", *Proc. LINAC'04*.
[4] T. Asaka *et al.*, "Performance of Electron Gun for SPring-8 Linac", *Proc. PAC'97*.
[5] T. Matsubara, *et al.*, PR ST-AB 9, 042801 (2006).
[6] A. Mizuno, linac group of SPring-8, private communication.
[7] Y. Kawashima, *et al.*, PR ST-AB 4, 082001 (2001).
[8] H. Hanaki, *et al.*, "Beam Stabilization in the SPring-8 Linac", *Proc. APAC'04*.
[9] Y. Shoji, "Estimation of Non-Linear RF Bucket of NewSUBARU", *Proc. SAST'03*, http://conference.kek.jp/sast03it/WebPDF/2P040.pdf.

ISBN 978-3-95450-119-9